

**COMPRESSIVE PROPERTIES AND SIMULATION OF LOW DENSITY
POLYETHYLENE FOAMS**

by

ZUNAIDA BINTI ZAKARIA

**Thesis submitted in fulfillment of the requirements
for the degree of
Doctor of Philosophy**

July 2013

ACKNOWLEDGEMENTS

First of all, *Alhamdulillah* and thank Allah for giving me strength and ability to complete this study.

First and foremost, my sincere gratitude and appreciation goes to my supervisor Assoc. Prof. Dr. Zulkifli Mohamad Ariff, for his guidance, criticism, ideas, encouragement and his enduring belief in my abilities throughout this research. Special thanks for the time he spent on editing to improve my thesis writing. Also my appreciation to my co-supervisor, Assoc. Prof. Dr. Azhar Abu Bakar because believe that I can do this research. I would like to express gratitude to Universiti Malaysia Perlis (UniMAP) and the Ministry of Higher Education for providing scholarship and funding my research. I also would like to thank the Centre for Knowledge, Communication & Technology for providing a SolidWorks server license which is essential for me to complete my research. Special thanks to my colleagues Dulan, Nadirah, Salmi, Houssein, and Norwanis for their guidance and support in many ways during this research. Thanks to Mr. Shahril, Mr. Segar, Mr. Faizal and Mr. Mohamad from School of Materials & Mineral Resources Engineering for their kindness and help during my research in the Rubber Laboratory, Plastics Laboratory and Latex Laboratory. I am gratefully thankful to my beloved husband, Mohamad Iskandar Azanan for his endless support and my daughter, Nur Syaza Qaisah for her smile. I appreciate the constant support, understanding and his encouraging words. Finally, my deepest gratitude is dedicated to my family for their love and ongoing support.

TABLE OF CONTENTS

ACKNOWLEDGEMENTS	ii
TABLE OF CONTENTS	iii
LIST OF TABLES	vii
LIST OF FIGURES	viii
LIST OF ABBREVIATIONS	xv
LIST OF SYMBOLS	xvi
ABSTRAK	xviii
ABSTRACT	xx
CHAPTER 1 : INTRODUCTION	1
1.1 Preamble	1
1.2 Problem statement	4
1.3 Research objectives	6
CHAPTER 2 : LITERATURE REVIEWS	8
2.1 Cellular solid	8
2.1.1 Polymeric foam.....	9
2.1.2 Metal foam.....	10
2.1.3 Ceramic foam.....	11
2.1.4 Syntactic foam	12
2.2 Polymer foam microstructure	13
2.2.1 Foam cell geometry	14
2.2.1(a) Relative foam density	15
2.2.1(b) Cell size.....	16
2.2.1(c) Cell shape	16
2.2.1(d) Cell wall thickness	17
2.3 Models of foam materials	17

2.3.1	Two dimensional Honeycomb	20
2.3.2	Three dimensional-Closed-cell and Open-cell foams.....	20
2.3.2(a)	Cubic cell as open cell.....	22
2.3.2(b)	Tetrakaidecahedral @ Kelvin cell model as closed-cell	24
2.4	Theoretical models of elastic deformation	25
2.5	Finite Element Analysis (FEA)	29
2.5.1	ABAQUS	30
2.5.2	SolidWorks	35
2.6	Mode of deformation	36
2.6.1	Tensile properties.....	36
2.6.2	Impact properties	37
2.6.3	Compression properties	38
2.7	Failure deformation mechanism	40
2.7.1	Tensile.....	41
2.7.2	Compression	41
2.8	Applications.....	45
2.8.1	Cushion packaging.....	47
2.8.2	Thermal insulation	47
2.8.3	Sport and leisure	48
CHAPTER 3 : MATERIALS AND METHODS		49
3.1	Introduction	49
3.2	Experimental.....	51
3.2.1	Raw materials	51
3.2.1(a)	Base polymer.....	51
3.2.1(b)	Blowing agent	51
3.2.1(c)	Activator.....	51
3.2.1(d)	Crosslinking agent.....	52
3.2.2	Formulation variation	52
3.2.3	Compounding	53
3.2.3(a)	Compound without BA	53
3.2.3(b)	Compound with BA	54
3.2.4	Compression molding.....	55
3.2.4(a)	Unblown matrix sample	55

3.2.4(b)	Foam sample	56
3.3	Sample characterization.....	56
3.3.1	Density	56
3.3.2	Cell structure.....	57
3.3.2(a)	Sample preparation for cell structure observation.....	59
3.3.2(b)	Effectiveness of black soot coating technique	60
3.3.3	Compression test.....	61
3.3.4	Real-time monitoring of compression deformation mechanism....	62
3.3.4(a)	Compression deformation	62
3.3.4(b)	Foam strain versus cell strain in compression deformation	64
3.3.4(c)	Effect of strain rate on compression deformation	66
3.4	Finite Element Analysis (FEA)	67
3.4.1	Foam cell model construction.....	67
3.4.2	Linear elastic analysis.....	69
3.4.3	Foam cell structural parameters.....	70
3.4.4	FEA Procedure.....	75
3.5	The comparison of FEA using Mills model and proposed model.....	75
3.6	Effective modulus theory.....	77
CHAPTER 4 : RESULTS AND DISCUSSION		78
4.1	Microstructures features	78
4.1.1	Simple image enhancement by black soot and Au/Pd coating	78
4.1.2	The implementation of image enhancement for structure characterization in relation to DCP concentration.....	83
4.2	Evaluation of the end properties of LDPE foams.....	85
4.2.1	Effect of DCP concentration on relative density of LDPE foams .	86
4.2.2....	Effect of DCP concentration on compressive stress of LDPE foams	87
4.2.3	Study of compression deformation mechanism.....	91
4.2.3(a)	Effect of density and microstructure on the compressive response of LDPE foam.....	94
4.2.3(b)	Effect of compression direction and sample thickness on the compressive response of LDPE foam.....	101

4.2.3(c)	Effect of strain rate and density on the compressive response of LDPE foam.....	107
4.3	Finite element analysis (FEA) of foam cell deformation	114
4.3.1	Effect of the cell size in relation to DCP concentration on the models	116
4.3.2	Effect of cell wall thickness on the models	127
4.3.3	Effect of mesh density on the models.....	131
4.3.4	Effect of multiple cells on the models	136
4.4	Deformation mechanisms via finite element analysis (FEA) utilize Mills model and proposed model	143
4.5	The elastic modulus theory.....	153
CHAPTER 5 : CONCLUSIONS.....		160
5.1	Conclusion.....	160
5.1.1	Physical and mechanical features	160
5.1.2	Finite element analysis (FEA) of foam cell deformation	161
5.1.3	deformation mechanisms via Finite Element Analysis (FEA) utilized Mills model and proposed model	162
5.1.4	The elastic modulus theory.....	162
5.2	Recommendations for future research.....	163
REFERENCES.....		164
APPENDICES		
APPENDIX A		
APPENDIX B		
APPENDIX C		

LIST OF TABLES

		Page
Table 2.1	Virtual 3D geometric, discrete (Voxel) and structural unit cell and RVE structures	19
Table 2.2	The structural parameters for the three cell shapes of foam structure	21
Table 3.1	Formulation of compound with blowing agent	53
Table 3.2	Experimental data used in Solidworks simulation	71
Table 3.3	Tetrakaidecahedral cell models with different geometry	71
Table 3.4	Tetrakaidecahedral cell models with different thickness	72
Table 3.5	Tetrakaidecahedral cell models with different mesh densities	72
Table 3.6	Tetrakaidecahedral cell models with different multiple cells model	74
Table 4.1	The average cell size for rise direction and perpendicular to rise direction	96
Table 4.2	The properties of solid polymer and geometrical features of the LDPE foams	107
Table 4.3	Computation of the LDPE foams with different cell size, D and cell wall thickness, δ	115
Table 4.4	Compression stress (σ_y) of model in Y-direction	116
Table 4.5	Computation of the LDPE foams with cell wall thickness, δ	119
Table 4.6	Computation of the LDPE foams with different mesh size	123
Table 4.7	Computation of the LDPE foams with different multiple cells	129
Table 4.8	The values obtained by experiment and the predicted values by using several of theoretical model	134
Table 4.9	Computation of the E1 and E2 models	138
Table 4.10	The geometrical and mechanical properties of LDPE foam	152
Table 4.11	The energy absorbed by three samples with different thickness	154

LIST OF FIGURES

		Page
Figure 1.1	Cellular structure of an open and closed-cell LDPE foams structure	2
Figure 2.1	Microstructure of (a) ENR-25 foam, (b) LDPE foam, (c) Al foam, (d) Ni foam, (e) ceramic foams and (f) EPDM foam	8
Figure 2.2	Microstructure of (a) glass microballon+epoxy matrix (b) epoxy syntactic foam filled with epoxy hollow spheres (ESF/EHoS)	12
Figure 2.3	The properties of materials depend on the material of the cell walls, cell topology, and relative density	14
Figure 2.4	Virtual 2D and RVE structures (a) geometric, (b) discrete (pixel) and (c) structural unit cell	19
Figure 2.5	A two-dimensional undeformed honeycomb	20
Figure 2.6	Illustrations of the various shape of cells structure of foams	21
Figure 2.7	Dimensional analysis of open-cell foam (a) undeformed cell (b) linear elastic strut bending	23
Figure 2.8	Packing of three tetrakaidecahedron in a body-centered-cubic	24
Figure 2.9	(a) Mesh configuration of foam cell using beam and shell elements (b) Comparison of FE simulated and experimental data for compressive modulus	30
Figure 2.10	The model assembly used to simulate the dynamic response of virtual EPS foam	31
Figure 2.11	Comparison of experimental and modeled strain rate effects for 30 kg/m ³ EPS foam	32
Figure 2.12	Schematic of loading of (a) Voronoi model (b) tetrakaidecahedral model	32
Figure 2.13	Contours of equivalent plastic strain in uniaxial-compressed PS49 foam	33
Figure 2.14	Contours level of impact compression on EPS foam in [111] direction (a) initial plasticity, (b) 2 plastic hinges, (c) with hinges or developing hinges arrowed, (d) face contact	34

Figure 2.15	(a) Model of pyramid foam (b) meshing of undeformed pyramid with mirror symmetry (c) contour of compression	35
Figure 2.16	Typical stress-strain curve for tensile response of PVC foams with different densities	37
Figure 2.17	Typical curves impact test for foam materials	38
Figure 2.18	Schematic compressive stress-strain response of (a) elastomeric foam (b) elasto-plastic foam	39
Figure 2.19	Progressive deformation mechanism a) initial homogeneous deformation, b) strain localization at the upper end of specimen c),d) propagation to the underlying layers e) back to homogeneous deformation	42
Figure 2.20	EPS microstructure under different levels of compression (a) 0 %, (b) 3 %, (c) 30 %, (d) 60 %	43
Figure 2.21	Schematic of μ -CT with <i>in-situ</i> compression	43
Figure 2.22	Microstructure from <i>in-situ</i> μ -CT a) Undeformed, b) Initial linear elastic region, at 2% strain, c) Cells change shape at 4% strain, d) Immediately after first collapse in the stress-strain curve at 9% strain, e) Visible shear band at strain of 57%, f) Flattening with residual cells (strain of 68%), g) Densified foam structure at compressive strain of 74%	44
Figure 2.23	Reconstruction after segmentation in 3D, where a slice at an arbitrary position (in y-direction) is taken for which multiple 2D models are obtained	45
Figure 2.24	Main applications of polyethylene foams	46
Figure 2.25	Products of PE foams	46
Figure 3.1	Flow chart of preparation and characterization of LDPE foams	49
Figure 3.2	Schematic showing the heated two-roll mill for compounding process	54
Figure 3.3	Morphology of cell size by optical microscope at 200X magnification	58
Figure 3.4	Morphology of cell wall thickness by scanning electron microscope at 200X magnification	58
Figure 3.5	Schematic showing the preparation of black soot coating using kerosene lamp	59

Figure 3.6	The effect utilization of black soot coating on sample (a) without black soot (b) with black soot	60
Figure 3.7	Schematic showing the compression test machine	61
Figure 3.8	Photographic view of the experimental set up for real-time monitoring of compressive deformation mechanism	63
Figure 3.9	Schematic diagram of compression test for bottom-to-top direction	64
Figure 3.10	The strain of (a) LDPE foam (bulk sample) and (b) cells foams	65
Figure 3.11	Tracking of the markers of the cells strain during compression	66
Figure 3.12	Tetrakaidecahedron unit cell	68
Figure 3.13	Pop-up menu for Solidworks simulation feature manager	70
Figure 3.14	Graphical representation of tetrakaidecahedral cell models designed by experimental result	72
Figure 3.15	Graphical representation of tetrakaidecahedral cell models with different cell wall thicknesses	72
Figure 3.16	Graphical representation of tetrakaidecahedral cell models with different mesh densities for the same model	73
Figure 3.17	The multiple cell models with 4 cuboids sizes (12, 27, 48 and 75 cells)	74
Figure 3.18	Tetrakaidecahedral model (a) Mills model and (b) proposed model in BCC lattice direction	76
Figure 4.1	Captured micrographs of LDPE foam cells a) uncoated and b) coated with black soot under polarized light	79
Figure 4.2	Optical micrographs of a) Au/Pd coating and b) black soot coating	80
Figure 4.3	Micrograph of a) Au/Pd and b) black soot coating with polarized light	81
Figure 4.4	Cell size distribution of the LDPE foam with 1.5 phr DCP measured by SEM and OM	82
Figure 4.5	Optical micrographs of LDPE foam with different DCP concentrations	84

Figure 4.6	Effect of DCP concentrations on average cell size of LDPE foams	85
Figure 4.7	Effect of DCP concentration on relative density of LDPE foams	86
Figure 4.8	Effect of DCP concentration on stress-strain characteristics of LDPE foams	88
Figure 4.9	Effect of DCP concentration on compressive modulus of LDPE foams	89
Figure 4.10	LDPE foam produced at 175°C foaming temperature with 2.0 phr of DCP in its formulation	90
Figure 4.11	Optical micrograph of LDPE foam with a density of 55.8 kg/m ³ under different levels of compression	92
Figure 4.12	Compressive stress –strain curve at different relative density (LDPE0.5, $\rho_f/\rho_s= 0.064$) and (LDPE1.0, $\rho_f/\rho_s=0.074$)	95
Figure 4.13	SEM micrograph of strut cross section and cell wall thickness of a) LDPE0.5 and b) LDPE 1.0	96
Figure 4.14(a)	Progressive deformation mechanisms of LDPE0.5 during compression and their intensity color contour ($\rho_f = 55.8$ kg/m ³) a)initial undeformed state, b) 4% strained, c) 20% strained, d) 40% strained, and e) 60% strained	98
Figure 4.14(b)	Progressive deformation mechanisms of LDPE1.0 during compression their intensity color contour ($\rho_f = 64.0$ kg/m ³) a)initial undeformed state, b) 4% strained, c) 20% strained, d) 40% strained, and e) 60% strained	99
Figure 4.15	Cells strain versus foam strain for LDPE 0.5 and LDPE1.0 foams	100
Figure 4.16	Compressive strain of LDPE foams at different loading for a) top-to-bottom and b) bottom-to-top	102
Figure 4.17	Optical micrograph of the effect top-to-bottom compression on the cell's location a) top, b) center, and c) bottom at 0% of strain and 20% strain	104
Figure 4.18	Compressive strain of LDPE foam (64.0kg/m ³) at different sample thickness	105
Figure 4.19	Compressive stress of LDPE foam at different sample thickness	106

Figure 4.20	Compressive stress behaviour of LDPE foam (64kg/m^3) at different strain rate	108
Figure 4.21	Energy absorption of LDPE foams (64 kg/m^3) at different strain rate	110
Figure 4.22	Stress strain rate response of LDPE foam (64 kg/m^3)	111
Figure 4.23	Variation of the collapsed stress as a function foam density for different strain rate	112
Figure 4.24	Compressive stress of various density LDPE foam at strain rate 4×10^{-2}	113
Figure 4.25	The optical micrographs of LDPE foam with a density of 55.8kg/m^3 in different direction a) rise direction and b) perpendicular to the rise direction	114
Figure 4.26	Contour of von Mises stress for three tetrakaidecahedral models with different cell wall thickness and cell size for model a) A1, b) A2 and c) A3 and their crosssectional views	118
Figure 4.27	Compressive stress-strain curve of LDPE foam at different DCP concentrations (0.5, 1.0 and 1.5 phr)	119
Figure 4.28	The von Mises stress and Max Displacement of LDPE foam models with different cell size, D and cell wall thickness, δ	121
Figure 4.29	Contour of SY:Y Normal stress (σ_y) on tetrakaidecahedral models with different cell wall thickness and cell size for model a) A1, b) A2 and c) A3	122
Figure 4.30	Contour of SY:Y Normal strain (σ_y) on tetrakaidecahedral model of A1 at different level of compressive strain a) undeformed, b) 11% of strained, c) 30% of strained, and d) 50% of strained	124
Figure 4.31	The regional data for parametric distance evaluation	125
Figure 4.32	The von Mises stress (Pa) versus parametric distance of LDPE foam models with different cell size, D and cell wall thickness, δ	126
Figure 4.33	The displacement (m) versus parametric distance of LDPE foam models with different cell size, D and cell wall thickness, δ	126

Figure 4.34	Contour of von Mises stress for the three tetrakaidecahedral models with different cell wall thickness a) B1 (5 μm), b) B2 (10 μm), and B3 (15 μm)	128
Figure 4.35	Contour of SY:Y Normal stress (σ_y) on tetrakaidecahedral models with different cell wall thickness a) B1 (5 μm), b) B2 (10 μm), and c) B3 (15 μm)	130
Figure 4.36	The von Mises stress and displacement at different cell wall thickness	131
Figure 4.37	Contour of von Mises Stress within tetrakaidecahedral models with different mesh densities a) C1 (0.010 mm), b) C2 (0.015 mm), and c) C3 (0.020 mm)	133
Figure 4.38	Contour of SY:Y Normal stress (σ_y) on tetrakaidecahedral models with different mesh density a) C1 (0.010 mm), b) C2 (0.015 mm), and c) C3 (0.020 mm)	135
Figure 4.39	The von Mises stress and displacement versus No. of elements at different mesh density	136
Figure 4.40	Contour of equivalent strain of multiple cells models a) D1 (with 12 cells), b) D2 (with 27 cells), c) D3 (with 48 cells) and d) D4 (with 75 cells)	137
Figure 4.41	The multiple cells model relocated at same compression level 1.439×10^{-3} of strained a) D1, b) D2 c) D3 and d) D4	140
Figure 4.42	Contour of equivalent strain D4 for a) undeformed and b) deformed models at 20% of strain	141
Figure 4.43	Contour of SY:Y Normal stress (σ_y) on tetrakaidecahedral models with different cuboid sizes a) D1, b) D2, c) D3, and d) D4	142
Figure 4.44	Contour of equivalent strain in uniaxial-compressed single cell LDPE foams at different continuous path between the loads and restrain	144
Figure 4.45	Cuboid model of LDPE foams in uniaxial compression	145
Figure 4.46	Contour of equivalent strain in uniaxial-compressed LDPE foams at different continuous path between the loads and restrain	145
Figure 4.47	Contours of a) equivalent strain and b) normal strain Y-direction of LDPE foams with differences thickness in compression lattice [010] direction	147

Figure 4.48	The comparison of deformation mechanism between a) LDPE of 55.8 kg/m ³ produced in this study at 88% of strain and b) EPS of 49 kg/m ³ by Mills at 88% of strain	148
Figure 4.49	Contours of equivalent strain of LDPE foams at different compressive strain a) undeformed, b) 5% of strained, c) 30% of strained, d) 50% of strained, and e) 88% of strained in compression lattice [010] direction	149
Figure 4.50	Contour of a) von Mises stress, b) equivalent strain and c) normal strain Y-direction of E2 model in [010] compression lattice direction	151
Figure 4.51	Comparison between the prediction of different models and the experimental values of the Young's modulus LDPE foams	155
Figure 4.52	The cell walls and cell edge of low density polyethylene foams a) 0.5 phr DCP and b) 1.5 phr DCP	158

LIST OF ABBREVIATIONS

ADC	Azodicarbonamide
Au/Pd	Gold/Palladium
BA	Blowing agent
BCC	Based Centred Cubic
CAD	Computer Aided Design
DCP	Dicumyl Peroxide
EPDM	Ethylene propylene diene monomer rubber
FEA	Finite Element Analysis
LDPE	Low Density Polyethylene
OM	Optical Microscope
PE	Polyethylene
phr	Part per hundred rubber
SEM	Scanning Electron Microscope
SG	Specific gravity
UTM	Universal testing machine
UV	Ultra Violet
ZnO	Zinc Oxide

LIST OF SYMBOLS

D	Cell size
ρ_f	Density of foam material
ρ_s	Density of solid material
R	Relative density
E_f	Young's modulus of foam material
E_s	Young's modulus of solid material
δ	Thickness of the cell wall
σ_y	Yield strength
W	Weight
ε_f	Strain of foam
ε_c	Strain of cell
L	Length of deformation
L_{f°	Original length of the foam thickness
L_{c°	Original length of cell size
$\dot{\varepsilon}$	Strain Rate
T_g	Glass-transition temperature
ω	Frequency
t	Sample thickness
SY:Y	Normal stress in Y-direction
Hz	Hertz
s	Seconds

$^{\circ}\text{C}$	Degree Celsius
MPa	Mega Pascal
kPa	Kilo Pascal
kg	Kilograms
kg/m^3	Kilograms per cubic meter
mm	Millimeter
μm	Micrometer
N/m^2	Newton per meter square

SIFAT-SIFAT MAMPATAN DAN SIMULASI BUSA POLIETILENA BERKETUMPATAN RENDAH

ABSTRAK

Penyelidikan ini dijalankan untuk mengkaji ciri-ciri mampatan dan simulasi bagi busa polietilena berketumpatan rendah. Penyebatan sampel telah dilakukan dengan menggunakan termostat penggiling berpenggulung dua panas dan pembusaan menggunakan pengacuanan mampatan secara proses pembusaan peringkat tunggal pada 175°C. Sebatian disediakan dengan mengubah kepekatan dikumul peroksida (DCP) (iaitu 0.25, 0.5, 0.75, 1.0, 1.25, 1.5, 1.75 dan 2.0 bsg) untuk menilai kesannya ke atas struktur dan sifat-sifat mekanik. Sampel yang disediakan telah dicirikan melalui ketumpatan, morfologi sel (iaitu, saiz sel dan ketebalan dinding sel) dan ujian mampatan. Didapati ketumpatan relatif meningkat dengan peningkatan kepekatan DCP dan hal ini seterusnya mengakibatkan penurunan saiz sel dan peningkatan ketebalan dinding sel. Dalam ujian mampatan, modulus elastik meningkat dengan peningkatan kepekatan DCP. Mekanisme canggaan mampatan dilaksanakan dengan merakam imej dan memantau perubahan masa sebenar semasa ujian mampatan. Lenturan setempat dan pembengkokan dinding sel dalam kawasan elastik, keruntuhan sel dalam kawasan pemampatan dan jalur ricih diperhatikan dalam busa. Jalur ricih dengan kawasan berketumpatan tinggi ditemui serenjang dengan arah pembebanan dan ia disumbangkan oleh keruntuhan sel. Pemodelan dan simulasi telah berjaya dilaksanakan menggunakan pakej perisian SolidWorks. Untuk model yang dibina dengan bantuan keputusan eksperimen, sel yang besar mengalami sesaran tinggi dan tegasan von Mises yang rendah. Hal ini adalah disebabkan oleh sel

yang lebih besar dengan dinding sel nipis boleh dimampatkan dengan daya yang kurang dan perkara yang sebaliknya berlaku untuk sel kecil dengan dinding sel yang tebal. Keputusan juga menunjukkan sesaran dan tegasan von Mises menurun dengan peningkatan ketebalan dinding dan ketumpatan jejaring sel model. Untuk penggandaan sel dalam model yang dibangunkan, didapati sesaran menurun dan tegasan von Mises meningkat dengan peningkatan saiz kuboid. Beberapa persamaan matematik berkenaan dengan teori modulus elastik telah dikaji melalui perbandingan kajian ini dengan kajian sebelumnya oleh penyelidik lain. Keputusan menunjukkan persamaan yang dijana melalui eksperimen didapati mempunyai kesamaan yang baik dengan model yang dicadangkan oleh Mills dan Zhu.

COMPRESSIVE PROPERTIES AND SIMULATION OF LOW DENSITY POLYETHYLENE FOAMS

ABSTRACT

This research was conducted to study the compression properties and simulation of low density polyethylene foam. Samples compounding was done using thermostatically controlled heated two roll mill and foamed using a compression moulding via a single stage foaming process at 175°C. The compounds were prepared by changing dicumyl peroxide (DCP) concentration (i.e. 0.25, 0.5, 0.75, 1.0, 1.25, 1.5, 1.75 and 2.0 phr) to evaluate its effect on structure and mechanical properties. The prepared samples were characterized through density, cell morphology (i.e. cell size and cell wall thickness) and compression test. It was observed that the relative density increased with increasing DCP concentration and this subsequently decrease the cell size and increase the cell wall thickness. In compression test, results indicated that the elastic modulus increased with increasing DCP concentration. The compression deformation mechanisms were implemented by capturing the image and recording the real-time changes during compression test. The localized bending and buckling of the cell walls in elastic region, cells collapse in densification region and shear band were observed in the foam. The shear band with high density region was discovered in perpendicular to loading direction and it was contributed by cells collapse. The modelling and simulation part were successfully performed using SolidWorks software package. For models that were constructed with the assistance of experimental results, the larger cell model experienced high displacement and low von Mises stress. This is attributed to the

larger cell with thinner cell walls can be compressed with less force and vice versa for small cell with thicker cell walls. Results also indicated that displacement and von Mises stress decreased with increasing the wall thickness and mesh density of cell model. For the multiplication of cells in the constructed model, it was found that displacement decreased and von Mises stress increased with increasing cuboid size. A few mathematical equations regarding elastic modulus theory was studied by comparing the present results with previous studies by other researchers. The experimental generated equation was found to be in good agreement with the model proposed by Mills and Zhu.

CHAPTER 1

INTRODUCTION

1.1 Preamble

Recently, reducing amount of materials utilization in many applications are highly favourable due to environmental problem such as unmanageable solid waste. Therefore, the use of light weight materials such as foamed materials would utilize less material and could indirectly contribute to the reduction the solid waste tonnage. Polymeric foamed materials are invented to assist humanity in reducing the utilization of solid materials and they are extensively used in various applications due to their unique properties. Compared to unfoamed polymers (i.e. solid polymer), polymer foams have relatively superior mechanical properties such as high impact stress, toughness, high stiffness-to-weight ratio, high fatigue life (Wang *et al.*, 2010), kinetic energy absorbers and more important, it has special properties such as light weight, heat insulation and buoyancy. Because of these properties, polymer foams have been commercially applied in many applications such as packaging, agriculture, automotive, sport and leisure, etc.

Low density foam have found their applications more in protective packaging where it can offer safety of goods in transit and in personal protective equipment (Gibson and Ashby, 1988); this is due to the capability of this kind of foam to absorb energy. Low-density polyethylene (LDPE) foam products are widely used and among the most popular in polymer foam applications. This foam has been commercial interest and widely used in packaging, construction, sport and leisure as

well as transportation. In order to make LDPE foam applicable in various applications, it should have excellent properties. Foam properties are usually dependent on density, mechanical properties of base polymer and foam morphology structure that includes cell size, cell size distribution, cell wall thickness and cell shape. There are two types of cellular structures which are open-cell and closed-cell structure. However, the closed-cell structures have higher dimensional stability, low moisture absorption coefficients and higher strength compared to open-cell structure. Therefore, in this study LDPE foam with closed-cell structure will be produced and analyzed. Figure 1.1 displays examples of open and closed-cell LDPE foam structures.

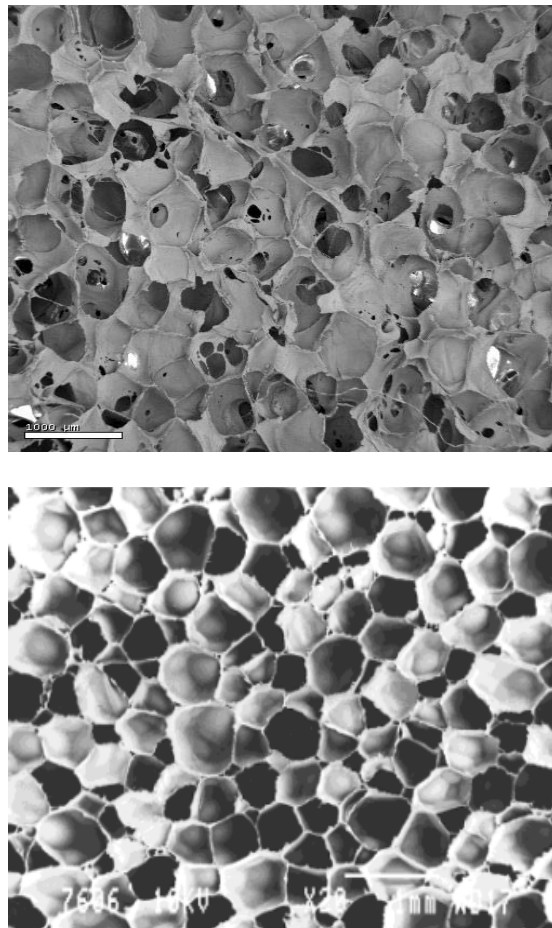


Figure 1.1 Cellular structure of an open and closed-cell LDPE foams
(Rodríguez-Pérez, 2005; Rodríguez-Pérez *et al.*, 1999)

Foam structures may be controlled by various parameters such as type of base polymer, blowing agent concentration, crosslinking agent level and processing conditions. Antunes and co-workers (2009) have reported similar statement where processing and foaming may strongly affect polymer foam morphology. In this study, in order to investigate variation in mechanical properties of LDPE foam, crosslinking agent concentration was varied. A common peroxide crosslinking agent was used, which is dicumyl peroxide (DCP) to tailor properties of the prepared LDPE foams. Different level crosslinking are needed for different applications, and DCP is an effective and economical crosslinking agent commonly used in the production of LDPE foams. In addition, crosslinking is an important way to improve the melt strength, thermal and chemical resistance of polymer foams (Liu *et al.*, 2011). Furthermore, Tai (2005) reported in his study that crosslinking help to promote the polymer melt strength (increase the molecular weight). Melt strength is needed to withstand the high pressure from blowing agent and stabilize the expanding bubbles. Therefore, crosslinking agent was utilized to increase bubble stabilization thus improve the properties of foams.

The application of polymer foams depends on its microstructure. Hence, to understand this behaviour, the mechanical properties such as their compression response need to be fully understood (Mills *et al.*, 2009). To be able to describe a specific mechanical behaviour of polymeric foams, modelling and simulation are sometimes required to predict unobservable mechanism of material deformation. Hence, predictive simulation in revealing the mechanical properties of polymer foams (i.e. microcellular foam) have been of great interest to researchers in recent years because of their unique microstructure (Mills, *et al.*, 2009; Kiernan and

Gilchrist 2010; Mills 2010; Viot *et al.*, 2010; Wang *et al.*, 2010). Beside simulation, Gibson and Ashby (Gibson and Ashby 1997) developed analytical foam models based on idealized single cell geometry to describe the foam mechanical response. Example of such system is the Kelvin foam structure, which was examined in ordered and in randomized versions by various authors (Dement'ev and Tarakanov 1970; Warren and Kraynik 1997; Zhu *et al.*, 1997; Gibson and Ashby 1997). Therefore, it is important to utilize predictive software package or modelling in order to predict the product properties before production. Even when modelling and simulation tend to be applied, experimental results from prototypes are still desired to study the actual performance during service. Therefore in this study, monitoring of experimental compression deformation mechanism are conducted and recorded in order to understand the real situation occurred within the cells structure. Attention is focused on cells structure and all the results related with the mechanical properties are presented in this study. Furthermore, LDPE foam is well-known to be applied in energy absorption applications such as packaging, cushioning and thermal insulation in floor (Rodríguez-Pérez *et al.*, 1999). Therefore, it is necessary to understand the foam deformation mechanism under various compressive deformations.

1.2 Problem statement

Currently, the production and utilization of LDPE foams has been focused significantly in various product and applications. LDPE foams are widely used in various applications and most popular among plastic foams. However, there are still limited studies of their cell structure response towards the mechanical deformation. Studies of tensile behaviour are quite common for solid polymer but it is rarely done for foams. This is partly due to the difficulty of sample gripping during testing and

the fact that foams are seldom subjected to tensile deformation during service. In contrast, compressive loading occurred predominantly during foams applications, for examples in packaging, cushioning and thermal insulation for floor foams are loaded by weight of the contents. Therefore, the study of compressive behaviour is the best way to understand the mechanical behaviour of polymer foams. This study was motivated by a need to understand foam microstructure response upon compression stress application. Therefore, in this study, the cell structure deformation during compression test is investigated and evaluated. In addition, most of the research works focusing on dynamic and high strain rate applications especially for polyurethane foam, epoxy foam and metal foam (Saha *et al.*, 2005; Oullet *et al.*, 2006 ; Subhash *et al.*, 2006; Sarva *et al.*, 2007), and very limited studies were conducted for LDPE foam although it is widely used in various industries and applications. Therefore, better understanding on the effects of cross-head speed or strain rate towards the foams mechanical response need to be evaluated, since LDPE foam experienced various compression rates in packaging, cushioning and thermal insulation in floor applications. The application of foams was also highly dependent on the cell structure and to address this matter, a few studies of this area have been done but there are still a lot of gaps to be filled. The cell structure of LDPE foam is flexible and it has tendency to return to its original dimension. The recovery is difficult to control and due to this problem most researchers decided to use *in-situ* μ -CT Imaging (Daphalapurkar *et al.*, 2008, Wisman *et al.*, 2010) and screw metal block (Vaitkus *et al.*, 2006) as methods to study the cell structure properties during compression. However, in this study the portable optical microscope will be coupled with universal testing machine to study the real time change on cell structure during compression. Besides, there are also gaps in incorporating the microstructure factor

to the foam deformation mechanism with the assistance of modelling software package. Most of the research works utilize the ABAQUS and LS-DYNA software to simulate their foam structure (Gilchrist and Mills, 2001; Alvarez *et al.*, 2009; Mills *et al.*, 2009; Kiernan and Gilchrist, 2010; Mills, 2010; Song *et al.*, 2010). ABAQUS is more complex compared to other types software package and heavily used in commercial industry such as in aerospace and civil engineering. However, emerging software package like SolidWorks also offer powerful tools which are easy to used and understand, more users friendly and well established among users of CAD software in Malaysia. Therefore in this study, SolidWorks software package was utilized to analyze the mechanical response of polymer foam towards compressive deformation.

1.3 Research objectives

This thesis covers three aspects of research in mechanical response of LDPE foams, which is the experimental, simulation verification and theoretical modelling. In order to achieve these objectives, foam samples will be prepared and tested to examine the effect such as different concentration of crosslinking agent. The prepared samples are evaluated in terms of their physical and mechanical properties, such as relative density, morphology and compressive stress. Subsequently, results from the analyses will be used as input for the simulation procedure which is going to predict the deformation mechanism. Experimental verifications are also conducted to evaluate the mechanical response of the foam cells. For the simulation process, foam cell models are developed and then simulated under real application which is via static analysis using SolidWorks CAD system. The cell model of the polymer foam is constructed based on a tetrakaidecahedral cell unit. The simulation results

will then be verified with the experimental results. Next, the theoretical modelling will be done by comparing available mathematical equation proposed by previous researchers with results obtained from the prepared foams.

To summarize the above paragraph into objectives of this research, the following list are prepared:

1. To prepare LDPE foams and evaluate their properties through relative density, cell morphology (e.g cells size, cell walls thickness) and compressive stress.
2. To investigate and evaluate the real-time changes on cell structure of LDPE foam during compression test.
3. To develop foam cell models based on tetrakaidecahedral cell unit and validate the constructed model using SolidWorks CAD system.
4. To determine and compare the elastic properties of LDPE foam based on theoretical approaches with that of obtained from experimental procedure.

CHAPTER 2

LITERATURE REVIEWS

2.1 Cellular solid

Foams or cellular solids are three-dimensional cellular materials which are made from an interconnected network of the edges and faces of cells (Gibson and Ashby, 1988). Foams are new materials of high interest in a wide range of application areas. It can be produced from wide variety of matrices such as polymer, ceramic or metal base. Polymeric foams are the most frequent produced but ceramic and metal foams are also receiving numerous attentions recently. Figure 2.1 shows the example of cellular solid that has been produced from different matrices.

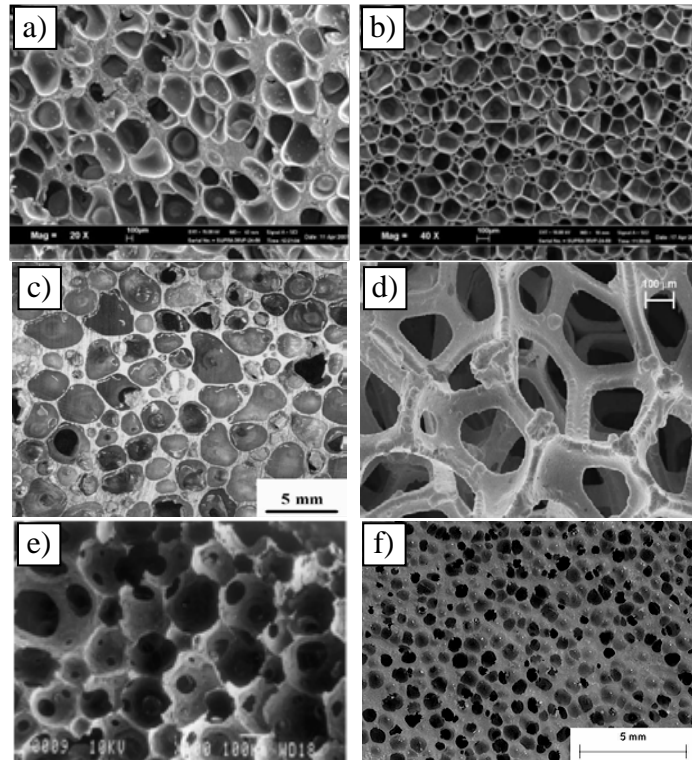


Figure 2.1 Microstructure of a) ENR-25 foam, b) LDPE foam, c) Aluminium foam, d) Nickel foam, e) ceramic foams and f) EPDM foam (Ariff *et al.*, 2008; Zakaria *et al.*, 2009; Mukai *et al.*, 2006; Jarrah *et al.*, 2005; Zakaria *et al.*, 2007)

2.1.1 Polymeric foam

Presently, the relevance of polymeric foams is continuously increasing due to their unique properties. Polymeric foam which often called cellular plastic have been studied for quite sometimes and it can be presented in the form of thermosetting, thermoplastic or elastomeric foams. Cellular plastics or plastic foams also referred to as expanded or sponge plastic and generally consist of a minimum of two-phases; a solid polymer matrix and a gaseous phase derived from blowing agent (Landrock, 1995). It has been used in the following major areas such as lightweight structure applications, energy absorption, sound absorption (Shu and Goh, 2001; Youssef *et al.*, 2005) thermal insulation, buoyancy and corrosion resistance (Wang *et al.*, 2009). Production of polymeric foams involves several steps which are compounding and foam formation. Usually to produce this type of foam, it needs several ingredients such as matrix (base polymer), crosslinking agent (can be chemical or physical such as radiation), blowing agent (chemical or physical) and several additional additives (such as processing aid, fillers, UV stabilizer, etc) (Rog  r  uez-P  rez, 2005). Generally, various techniques have been established to produce polymer foam according to the type of base polymer used. These techniques include extrusion, injection molding, compression molding and semi-continuous process which involve crosslinking by irradiation and chemical crosslinking.

Thermosetting foams can be defined as foams having no thermoplastic properties. Accordingly, thermosetting foams include crosslinked polymer foams and also linear polymeric foam which having no thermoplastic properties (such as polyimide foams). Most of the thermosetting foams are prepared by the simultaneous occurrence of polymer formation and gas generation. Whereas, thermoplastic foams

are more favorable than thermosetting foam due to its ease of processing and recyclable nature. Commercial thermoplastic foams that are currently produced include polystyrene (PS) foams which well known as expanded polystyrene (EPS) and also polyolefin foams such as low-density polyethylene (LDPE), high-density polyethylene (HDPE), linear low-density polyethylene (LLDPE), polypropylene (PP) and ethylene vinyl acetate copolymers (EVA) foams. Polyolefin foams are among the most commonly utilized commercial plastics foams and available in the market for various applications. LDPE foams are one type of polyolefin foams that are regularly used in many industries due to their excellent properties. The production of this foam usually involves thermal decomposition of a blowing agent at a specific temperature. Furthermore, the base polymer has an advantage of excellent resistance to most organic and inorganic chemicals. There are basically two types of LDPE foams that based on the approach of stabilizing the foam formation, i.e. extruded (cooling mechanism) and crosslinked. The extruded foam is produced in a continuous process, while the crosslinked foam can be prepared by batch or continuous process. Both of these foams have very similar chemical, mechanical and thermal properties (Landrock, 1995). Low-density polyethylene foams are used extensively in buoyancy and cushioning applications due to their predominantly closed cell structure. Therefore, the cell structure properties of LDPE foam are one of the major factors governing the performance of the foams and this factor is going to be evaluated extensively in this study.

2.1.2 Metal foam

Metal foams are structural materials in which gas bubbles are separated by thin metal walls and exhibit a unique combination of physical properties due to their

structure (Konstantinidis *et al.*, 2005). Metal foams offer advantages in terms of high specific strength, stiffness (Konstantinidis *et al.*, 2005) and temperature resistance (Shu and Goh, 2001). Metal foams are usually made by mixing organic beads into a metal melt in an inert atmosphere.

There are a lot of research works in metal foams that commonly focused on aluminium foams and it becomes apparent that aluminium is the largest metal matrix used to produce metal foams recently (Konstantinidis *et al.*, 2009; Rajendran *et al.*, 2009; Mu *et al.*, 2010; Nammi *et al.*, 2010). Nevertheless, there are also researches which studied on nickel foam (Jarrah *et al.*, 2005). Metal foams can have a closed-cell or open-cell structure depending on their blowing agent or foaming system. Mu and his co-workers (2010) have reported that the cell shape anisotropy can lead to anisotropy in mechanical properties either from closed-cell foam or open-cell aluminium foam. The applications of metal foams that has been given attention are mainly in impact energy absorbing components, decks and bulkheads, compressor casings, motorcycle exhaust and frames, submarine structures, acoustic transducers, biomedical implants, heat exchanger and battery electrodes (Shu and Goh, 2001; De Giorgi *et al.*, 2010; Konstantinidis and Tsipas, 2010).

2.1.3 Ceramic foam

Ceramic foam is a class of high porosity materials that are used for a wide range of technological applications (Muhamad Nor *et al.*, 2008). It can be made from a wide range of ceramic materials, where both oxide and non-oxide can be utilized to create various range of potential applications. Ceramic foam can be produced through polymeric sponge replication method. In this process, commercial polymeric

foam was used as a template and dipped into a ceramic slurry followed by drying and sintering to yield a replica of the original polymeric foam (Muhamad Nor *et al.*, 2008). There is another production technique of ceramic foam which is known as gel casting as reported by Ramay and Zhang (2003). The foams may consist of several ceramic materials such as aluminum oxide, a common high-temperature ceramic that gets its insulating power from the many tiny voids within the material. It can be used not only for thermal insulation, but for a variety of other applications such as acoustic insulation, adsorption of environmental pollutants and as filtration of molten metal alloys.

2.1.4 Syntactic foam

A special class of closed-cell foams is known as syntactic foam, which consists of hollow particles embedded in a matrix material. It also can be defined as composite materials in which hollow microspheres or other small hollow particles, are randomly dispersed in a matrix (Puterman *et al.*, 1980). Basically, there are two types of syntactic foams; i.e. two-phase syntactic foam and three-phase syntactic foam (Samsudin *et al.*, 2011). Figure 2.2 shows the example of syntactic foams that have been produced by a few researchers.

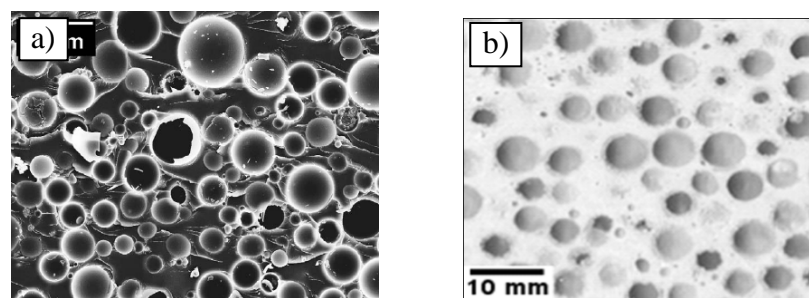


Figure 2.2 Microstructure of a) glass microballon+epoxy matrix and b) epoxy syntactic foam filled with epoxy hollow spheres (ESF/EHoS) (Gupta and Ricci, 2006; Samsudin *et al.*, 2011)

Hollow microspheres or spheres can be made from several materials, including glass, ceramic and polymers. Syntactic foams are known for their high specific compressive strength due to high strength-to-weight ratio, low moisture absorption and excellent damping properties. In addition, they can be considered as multi-functional composite materials due to their broad range of mechanical properties coupled with vibration damping characteristics, fire performance and ability to be fabricated in functionally graded configurations (Gupta, 2003). Presently, they are used in aerospace, automotive, civil as well as marine (deep-sea) structural applications (Tagliavia *et al.*, 2009).

2.2 Polymer foam microstructure

Polymer foams have various cell size and shapes which can be affected by crosslinking agent, blowing agent and processing parameter. The applications of polymer foams in the industries depend on their structure response upon on mechanical testing. Moreover, structural response of polymer foams strongly depends on foam density, cell structure such as cell size and cell type (i.e. open or closed-cell) and their base material properties (Saha *et al.*, 2005; Song *et al.*, 2010). Closed-cell low-density polymer foams are usually used for protective packaging of goods in transit and in personal protective equipment (Mills, 2007). Therefore, it is important to understand the real situation occurring in the foam cell structure during service. Generally, different cell size and cell wall thickness of the foam will influence the mechanical properties of particular foam as highlighted by Venkatachalam (2008) that the properties of foams are related to its structure and the properties of the matrix of which the cell walls and edges are made.

2.2.1 Foam cell geometry

In general, mechanical properties of closed-cell or open-cell of foams are dependent on the properties of matrix from which the foam is made and the cell geometry properties. Foam cell geometry plays an important role in the behaviour of foam (Shulmeister, 1998). Many studies have shown that the mechanical properties of foams are affected by the micro-structural parameters such as the relative density and their geometrical structure (i.e. cell size and cell morphology) (Roberts and Garboczi, 2001; Zheng *et al.*, 2005; Alvarez *et al.*, 2009; Wang *et al.*, 2010). Moreover, the mechanical properties can also be affected by the matrix of foam. Cells morphology is an important parameter that could affect the foam deformation mechanism and it can be categorized in terms of cell shape and cell wall thickness of the foam. Furthermore, Ashby (2006) has also made a summary in his previous study, where there are three dominant factors that influence cellular properties of foams as displayed in Figure 2.3. These factors include cell geometry such as cell topology and shape, relative density, cell wall thickness and cell edge length.

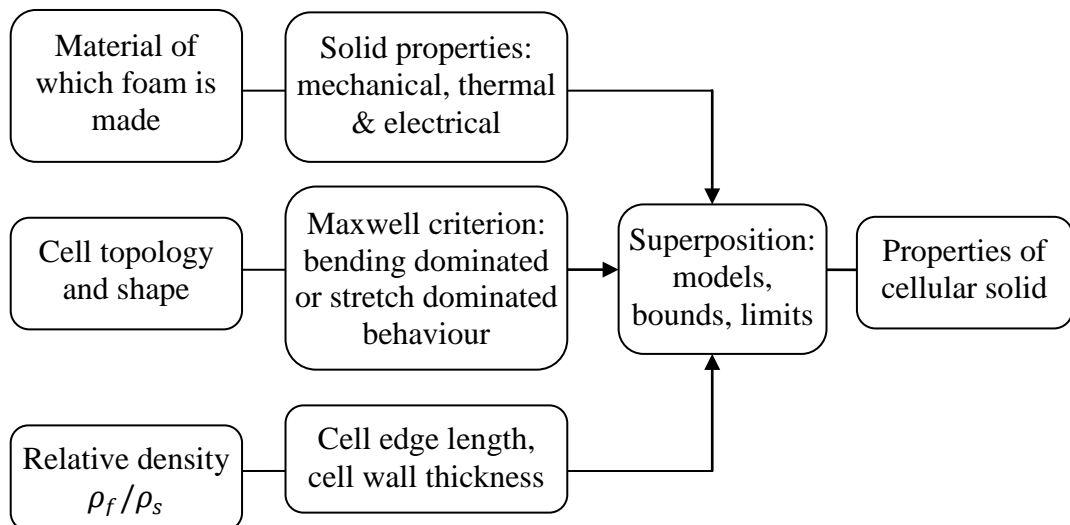


Figure 2.3 The properties of materials depend on the material of the cell walls, cell topology, and relative density (Ashby, 2006)

2.2.1 (a) Relative foam density

Most researchers used relative density as their main parameter for the prediction of the mechanical properties of foam cell structure (Zhang, 2007; Antunes *et al.*, 2009; Song *et al.*, 2010). It is important to link physical properties of cellular solids to their relative density of complex structure, in order to understand how such properties can be optimized to a given application (Roberts and Garboczi, 2001). The relative foam density can be calculated through ρ_f/ρ_s (ρ_f is the density of the foam and ρ_s is density of solid material) and it is a crucial parameter for the physical properties of foam. Relative density of foam is a very important parameter and its importance can be clearly observed when the foam is evaluated for mechanical, thermal and electrical performance during its applications.

The foam density, ρ_f , can be calculated by simply dividing the mass of the foam sample by its volume. There is also another method to measure ρ_f which is via the Archimedes principle that based on water displacement. The latter method is selected only if the cell structure of the foam is closed-cell. Density value is averaged from several samples, because the cellular structure of foam usually is not always homogeneous throughout the sample. This homogeneity can be affected by temperature differences during the foam production process which results in different foaming rates (Shulmeister, 1998).

For low density foams $0.05 < \rho_f/\rho_s < 0.20$ Gibson and Ashby (1988) reported that Young's modulus (E) of foam materials from experimental results is related to their density (ρ) through mathematical relationship which will be discussed later in the theoretical part. Moreover, Zhu *et al.* (2000) and Li *et al.* (2003; 2005) also

stressed the same point where the Young's modulus of foams is really dependent of their relative density.

Song *et al.* (2010) reported that with the increases of the relative density, the plateau stress increased and then the strength and stiffness of foams were enhanced for any given value of cell shape irregularity. They also reported that densification strain energy approximately increased linearly with the relative density. Therefore, it is important to note that mechanical properties of foam materials are heavily dependent on their relative density (Czekanski *et al.*, 2005).

2.2.1 (b) Cell size

Conventional 2D image analysis allows us to get a 2D cell size distribution. The cell size may be measured directly by inspection of foam cross-section (Eaves, 2001) and its distribution is very easy to obtain when the cells' area are perfectly closed (i.e. closed cell foam). The average cell size D is one of the important parameters related with foam geometry because it can indirectly influence the mechanical properties of the foams.

2.2.1 (c) Cell shape

Cell shape of foam materials can be irregular (i.e. Voronoi tessellation) or regular (i.e. tetrakaidecahedral cells) (Youssef *et al.*, 2005; Zhang, 2007). In order to study the mechanical behaviour of foams, researchers usually use a unit cell model with regular cell shape to determine the relationship between the basic mechanical properties and the cell structure parameter. The same approaches will also be used in this study where the tetrakaidecahedral cell will be the unit cell model.

2.2.1 (d) Cell wall thickness

Closed-cell foam can be generally described with edge and walls due to its cells are not connecting with the neighboring cells. The cell wall thickness is an important parameter which could affect on the final properties. Gibson and Ashby (1982) in their work reported that the cell wall property had a relationship with the relative density based on dimensional arguments. This was interpreted through a simple expression for the modulus and collapse strength, of the foam (Gibson and Ashby, 1982).

$$\frac{\text{Foam property}}{\text{Cell wall property}} = C \left(\frac{\rho_f}{\rho_s} \right)^n \quad (2.2)$$

where ρ_f/ρ_s is the relative density of the foam, and C and n are constants. Moreover, Mills and Zhu (1999) also reported that when relative density is low, the face thickness, δ_f is related to the face relative density, R by:

$$\delta_f = \frac{16lR}{3\sqrt{2} + 6\sqrt{6}} \quad (2.2)$$

where length of edge is l . This equation shows that the total of solid content in the cell wall thickness is also important and this could affect the mechanical properties of foam.

2.3 Models of foam materials

Cellular materials can be represented by a number of 2D and 3D micromechanical models that have been proposed by a few researchers (Zhu *et al.*,

1997). Honeycombs with regular unit repetition (i.e. prismatic cells) are referred as two dimensional cellular solids. However, foams with stochastic units (i.e. polyhedral cells) are three dimensional cellular solids (Gibson, 2005). The cellular structure may have regular or stochastic topologies depending on the distribution of solid phase. Vural (2005) has detailed out in his study, that cellular solid with stochastic topology have a tendency to exhibit isotropic properties, mainly due to random shape and cells orientation. Conversely, for the regular topology, it usually has anisotropic properties due to the presence of elongated prismatic cells in common practice. Furthermore, they are also affected by open-cell or closed-cell structure depending on the interconnectivity among individual cells. Both cellular structures can be classified as unit cell model.

Unit cell model or single cell level is used to study the micro-mechanics aspect which represents the behaviour of foam in terms of deformation occurring in the cell model. Tetrakaidecahedral cell is the most famous structure used to represent the open-cell and closed-cell foam behaviour. It is also known to be the only polyhedron that can be packed with identical units to fill space and have low surface energy (Demiray *et al.*, 2006; Venkatachalam, 2008; Wang *et al.*, 2009).











Venkatachalam (2008) also reported that the properties of the cellular solid are directly affected by the shape and structure of the cells and hence, the structure of the cells is very important. A single tetrakaidecahedral cell isolated from the foam material is usually used to represent the structural unit which is called Representative Volume Element (RVE). RVE model reproduced exactly real foams or idealized nature, since they consider mesoscopic features that directly affect the final

mechanical behaviour (Alvarez *et al.*, 2009). Figure 2.4 shows the virtual 2D geometry of a unit cell and its RVE structure while Table 2.1 shows the example of virtual unit cells in 3D geometry.



Figure 2.4 Virtual 2D and RVE structures a) geometric, b) discrete (pixel) and c) structural unit cell (Alvarez *et al.*, 2009)

Table 2.1 Virtual 3D geometric, discrete (Voxel) and structural unit cell and RVE structures (Alvarez *et al.*, 2009)

Element type	Geometric	Discrete(voxel)	Structural		
	Solid	Solid	Beam	Shell	Beam-shell
Unit cell(3D) Open cell				Non applicable	
Unit cell(3D) Closed- cell			Non applicable		
RVE 3D		Unreasonable resolution time			
ρ_f	$\rho_f > 0.5-0.6$	$0.5 > \rho_f > 0.008$ $0.5 > \rho_f > 0.1$	$\rho_f < 0.013$	$\rho_f < 0.148$	$\rho_f < 0.161$

2.3.1 Two dimensional Honeycomb

Two dimensional (2D) modelling of foam materials is often based on regular honeycomb microstructure as shown in Figure 2.5. Due to its six-fold symmetry (i.e. all sides of the same length and all internal angles are 120 degrees), a hexagonal unit cell exhibits isotropic mechanical behaviour as reported by Warren and Kraynik (1997). Moreover, among all 2D microstructures, the hexagonal unit cell partitions have large space-filling properties compared with other 2D shapes.

In honeycomb structure, loading along the prism axis, which is in the out-of plane direction will cause the cell walls to be initially compressed axially. This subsequently gives Young's modulus simply varies with the volume fraction of solid or with the relative density as reported by Gibson (2005).

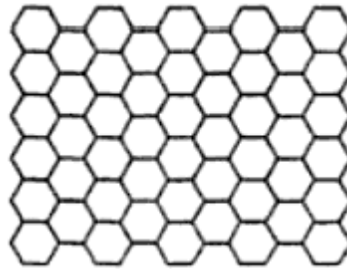


Figure 2.5 A two-dimensional undeformed honeycomb

2.3.2 Three dimensional –Closed-cell and Open-cell foams

2D models are severely limited to describe realistic characteristics of foams. Therefore, it is of great significance to develop three dimensional (3D) models for foam cells and investigate their compressive behaviour. 3D models are based on regular periodic micro-geometries which can be generated from space filling of regular polyhedral (Konstantinidis *et al.*, 2005). There are several regular polyhedral models such as tetrakaidecahedral, cubic and dodecahedral (Maruyama *et al.*, 2006)

as shown in Figure 2.6 and their structural parameters are shown in Table 2.2. Foam materials are totally different with the honeycombs, where the mechanical properties can be estimated base on their mechanisms of deformation and failure (Gibson, 2005). Gibson (2005) also assumed that the cell geometry of the cell foams with various relative densities is similar.

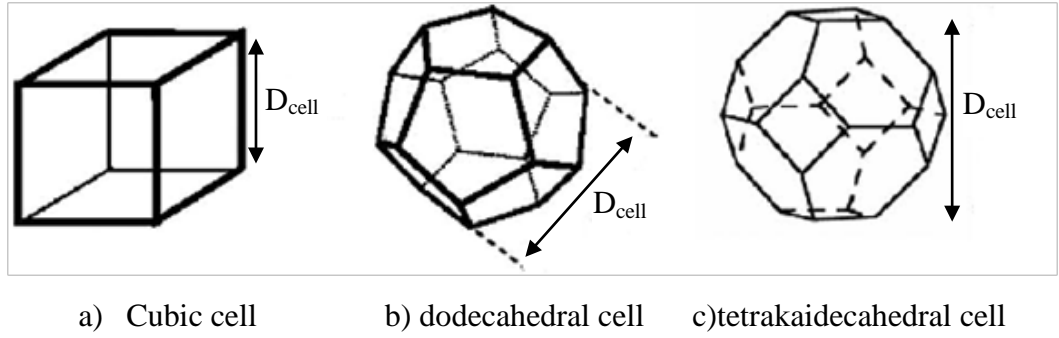


Figure 2.6 Illustrations of the various shape of cell structure of foams (Rémi *et al.*, 2009)

Table 2.2 The structural parameters for the three cell shapes of foam structure (Rémi *et al.*, 2009)

Cell	Cube	Dodecahedron	Tetrakaidecahedron
volume	$V_{\text{cube}} = D_{\text{cell}}^3$	$V_{\text{dode}} \approx 0.427 \times D_{\text{cell}}^3$	$V_{\text{tetr}} = 0.5 \times D_{\text{cell}}^3$
Window area	$S_{\text{win}} \approx D_{\text{cell}}^2$	$S_{\text{win}} \approx 0.251 \times D_{\text{cell}}^2$	$S_{\text{win},1} \approx 0.32476 D_{\text{cell}}^2$ (hexagon) $S_{\text{win},2} = 0.125 D_{\text{cell}}^2$ (square)
Cell total window area	$S_{\text{cube}} = 6 \times S_{\text{win}}$ $S_{\text{cube}} = 6 \times D_{\text{cell}}^2$	$S_{\text{dode}} = 6 \times S_{\text{win}}$ $S_{\text{dode}} \approx 3.0122 \times D_{\text{cell}}^2$	$S_{\text{tetr}} = 8 \times S_{\text{win},1} + 6 \times S_{\text{win},2}$ $S_{\text{tetr}} \approx 3.3480 \times D_{\text{cell}}^2$
Particles per unit volume	$N = \frac{3}{V_{\text{cell}}} = \frac{3}{D_{\text{cell}}^3}$	$N = \frac{6}{V_{\text{cell}}} \approx \frac{14.006}{D_{\text{cell}}^3}$	$N = \frac{4}{V_{\text{cell}}} = \frac{8}{D_{\text{cell}}^3}$ (hexagon) $N = \frac{3}{V_{\text{cell}}} = \frac{6}{D_{\text{cell}}^3}$ (square)
Relation $\varepsilon_{\text{cell}}/h$	$h = \frac{(1 - \varepsilon_{\text{cell}}) \times D_{\text{cell}}}{3}$	$h \approx 0.2836 \times (1 - \varepsilon_{\text{cell}}) \times D_{\text{cell}}$	$h \approx 0.29898 \times (1 - \varepsilon_{\text{cell}}) \times D_{\text{cell}}$

2.3.2 (a) Cubic cell as open cell

The cubic cell is the most important cell that has been used to represent mechanical properties of open-cell foam. Deformation for cubic cell model in the linear elastic regime is primarily characterized as bending of the cell edges. The Young's modulus, E_f can be estimated from the following equation in relation to deformation as shown in Figure 2.7(a) and Figure 2.7(b). Under a transverse load, F , the bending deflection, δ , of a strut of length, l , and cross-sectional area proportional to t^2 (refer Figures 2.7(a) and 2.7(b)) is reported by Gibson (2005):

$$\delta \propto \frac{Fl^3}{E_s t^4} \quad (2.3)$$

where E_s is the Young's modulus of the solid. The stress acting on the cell is proportional to F/l^2 and the strain is proportional to δ/l , giving:

$$\frac{E_f}{E_s} \propto \left(\frac{t}{l}\right)^4 \quad (2.4)$$

The relative density of any open-cell foam ρ_f/ρ_s , is proportional to the square of the ratio of the strut thickness to length, t/l , so that;

$$\frac{E_f}{E_s} = C_1 \left(\frac{\rho_f}{\rho_s}\right)^2 \quad (2.5)$$

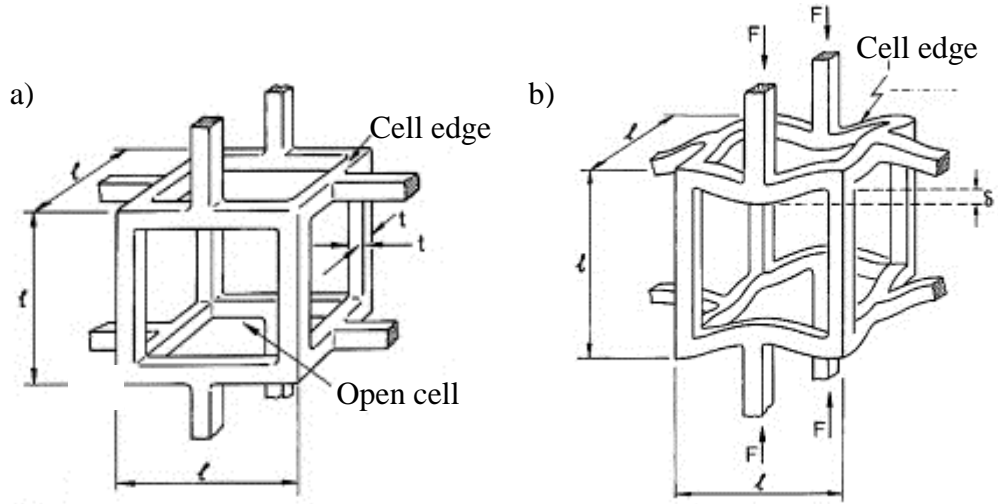


Figure 2.7 Dimensional analysis of open-cell foam a) undeformed cell and b) linear elastic strut bending (Gibson, 2005)

From Equation 2.5, it can be shown that the Young's modulus of the foam is dependent on the solid elastic modulus and foam relative density. Single constant, C_1 , is a combination of all of constants proportionally related to the cell geometry. This equation also could be used for closed-cell foam where it has been corrected by Gibson and Ashby (1982), which allow them to calculate the Young's modulus of closed-cell as;

$$\frac{E_f}{E_s} = C_1 \left(\frac{\rho_f}{\rho_s} \right)^3 \quad (2.6)$$

Both equations (i.e. Equation 2.5 and 2.6) are used for linear elastic behaviour of foam materials. For a cubic cell, the single constant $C_1 \sim 1$ is fitted to Equation 2.4, however, for the tetrakaidecahedral unit cell model the single constant is found to be $C_1 = 0.98$ (Warren and Kraynik, 1997). More information about tetrakaidecahedral unit cell model will be detailed out in Section 2.4.

2.3.2 (b) Tetrakaidecahedral @ Kelvin cell model as closed-cell

A few models have been used to model the closed-cell foam structure and usually different materials will give completely different shape of the unit cell model. It is difficult to define a representative unit cell for foam because foam has many irregularities such as different cell shapes, solid distribution and distribution of cell size (Simone and Gibson, 1998). The tetrakaidecahedral foam model, in particular, has been the subject in many recent studies (Fischer *et al.*, 2009; Song *et al.*, 2010; Wang *et al.*, 2010). The cells of the model are defined by truncating the corners of a cube giving eight hexagonal and six square faces as shown in Figure 2.8. This foam cell model relatively have a low anisotropy, and it is thought to be a good model of isotropic cellular solids (Roberts and Garboczi, 2001; De Giorgi *et al.*, 2010). The closed cell foam is found to be isotropic, whereas the semi-open cell foam showed strong anisotropy.

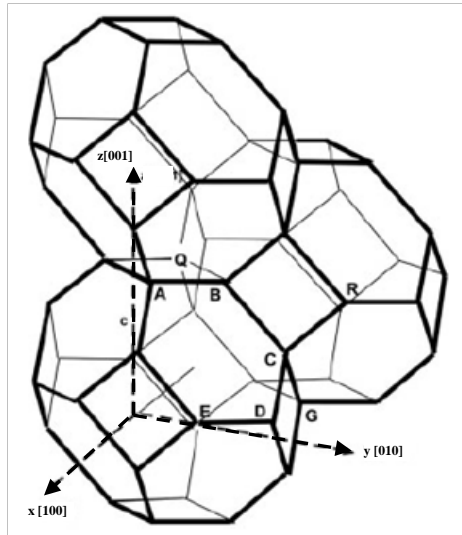


Figure 2.8 Packing of three tetrakaidecahedron in a body-centered-cubic (Almanza *et al.*, 2004)